Metabolic Engineering 61 (2020) 141–151

Contents lists available at ScienceDirect

Metabolic Engineering

journal homepage: www.elsevier.com/locate/meteng

Heterologous production of 3-hydroxyvalerate in engineered *Escherichia coli*

Dragan Miscevic[a], Kajan Srirangan[b], Teshager Kefale[a], Shane Kilpatrick[a], Duane A. Chung[a,c,d], Murray Moo-Young[a], C. Perry Chou[a,*]

[a] Department of Chemical Engineering, University of Waterloo, Waterloo, Ontario, N2L 3G1, Canada
[b] Biotechnology Research Institute, National Research Council of Canada, Montreal, Quebec, H4P 2R2, Canada
[c] Department of Pathology and Molecular Medicine, McMaster University, Hamilton, Ontario, L8S 4L8, Canada
[d] Neemo Inc., Hamilton, Ontario, L8L 2X2, Canada

ARTICLE INFO

Keywords:
Escherichia coli
Glycerol
3-Hydroxyacid
3-Hydroxyvalerate
Propionyl-CoA
Sleeping beauty mutase

ABSTRACT

3-Hydroxyacids are a group of valuable fine chemicals with numerous applications, and 3-hydroxybutyrate (3-HB) represents the most common species with acetyl-CoA as a precursor. Due to the lack of propionyl-CoA in most, if not all, microorganisms, bio-based production of 3-hydroxyvalerate (3-HV), a longer-chain 3-hydroxyacid member with both acetyl-CoA and propionyl-CoA as two precursors, is often hindered by high costs associated with the supplementation of related carbon sources, such as propionate or valerate. Here, we report the derivation of engineered *Escherichia coli* strains for the production of 3-HV from unrelated cheap carbon sources, in particular glucose and glycerol. Activation of the sleeping beauty mutase (Sbm) pathway in *E. coli* enabled the intracellular formation of non-native propionyl-CoA. A selection of enzymes involved in 3-HV biosynthetic pathway from various microorganisms were explored for investigating their effects on 3-HV biosynthesis in *E. coli*. Glycerol outperformed glucose as the carbon source, and glycerol dissimilation for 3-HV biosynthesis was primarily mediated through the aerobic GlpK-GlpD route. To further enhance 3-HV production, we developed metabolic engineering strategies to redirect more dissimilated carbon flux from the tricarboxylic acid (TCA) cycle to the Sbm pathway, resulting in an enlarged intracellular pool of propionyl-CoA. Both the presence of succinate/succinyl-CoA and their interconversion step in the TCA cycle were identified to critically limit the carbon flux redirection into the Sbm pathway and, therefore, 3-HV biosynthesis. A selection of *E. coli* host TCA genes encoding enzymes near the succinate node were targeted for manipulation to evaluate the contribution of the three TCA routes (i.e. oxidative TCA cycle, reductive TCA branch, and glyoxylate shunt) to the redirected carbon flux into the Sbm pathway. Finally, the carbon flux redirection into the Sbm pathway was enhanced by simultaneously deregulating glyoxylate shunt and blocking the oxidative TCA cycle, significantly improving 3-HV biosynthesis. With the implementation of these biotechnological and bioprocessing strategies, our engineered *E. coli* strains can effectively produce 3-HV up to 3.71 $g\,l^{-1}$ with a yield of 24.1% based on the consumed glycerol in shake-flask cultures.

1. Introduction

The increasing concerns surrounding climate change and fossil fuel depletion have sparked a growing interest for bio-based production of value-added chemicals and fuels from renewable feedstocks (Bevan and Franssen, 2006). Recent biotechnological progress, particularly in the areas of genetic/genomic engineering, synthetic biology, systems biology, and metabolic engineering, offers novel tools to customize cell factories for bio-based production (Nielsen and Keasling, 2016). Implementation of these tools can enhance the development of large-scale bio-based production processes, offering an economically feasible alternative to manufacturers (Erickson et al., 2012). In particular, pharmaceutical and drug companies are exploring more efficient and sustainable means for the production of fine chemicals without the use of expensive catalysts (e.g., precious metals), harsh physical conditions, and toxic solvents (Welton, 2015), as well as novel synthesis techniques that can overcome substrate specificity challenges and minimize by-products (Federsel, 2005). For effective bio-based production, it is thus critical to identify novel metabolic pathways generating target products at a high yield and selectivity for implementation in genetically robust microbial hosts (Jullesson et al., 2015).

3-Hydroxyacids are a group of valuable fine chemicals as potential

* Corresponding author. Department of Chemical Engineering, University of Waterloo, 200 University Avenue West, Waterloo, Ontario, N2L 3G1, Canada.
E-mail address: cpchou@uwaterloo.ca (C.P. Chou).

https://doi.org/10.1016/j.ymben.2019.11.005
Received 6 August 2019; Received in revised form 25 October 2019; Accepted 9 November 2019
Available online 12 November 2019

building blocks for the production of various antibiotics, vitamins, pheromones, and aromatic derivatives (Fonseca et al., 2019; Mori, 1981; Nahar et al., 2009; Toshiyuki and Takeshi, 1987), due to their structural nature containing two reactive functional groups, i.e., hydroxyl and carboxyl groups, and the reactivity of introducing an extra chiral carbon. Currently, industrial production of 3-hydroxyacids are primarily conducted via two chemical processes: i.e., (i) selective oxidation through Sharpless' asymmetric epoxidation and subsequent hydroxylation (Ren et al., 2010; Spengler and Albericio, 2014) and (ii) reduction of 3-ketoesters (Noyori et al., 2004). Additionally, chemical degradation of polyhydroxyalkanoates (PHAs), which are biopolymers naturally made in select microorganisms, via acid methanolysis, fractional distillation, and saponification, has been reported for the preparation of 3-hydroxyacids (de Roo et al., 2002). However, bio-based production of 3-hydroxyacids has recently gained attention due to the development of biocatalysts that can potentially enhance the structural variety, yield, and enantioselectivity of the product. Basically, bio-based production of 3-hydroxyacids is carried out in two ways: i.e., (i) depolymerization of PHAs in natural producing hosts (Anis et al., 2017; Biernacki et al., 2017) and (ii) direct biosynthesis in natural or engineered microorganisms (Tseng et al., 2009, 2010). Since biological depolymerization of PHAs is a complex and expensive approach, direct biosynthesis of 3-hydroxyacids is regarded as a more feasible option for industrial application. 3-Hydroxybutyrate (3-HB), the monomer of polyhydroxybutyrate (PHB), represents the most common 3-hydroxyacid. Structurally, 3-HB can be directly biosynthesized via Claisen condensation of two acetyl-CoA moieties to form acetoacetyl-CoA followed by subsequent reduction and CoA removal (Figs. 1 and 2), and the associated key enzymes, e.g., acetoacetyl-CoA thiolase (PhaA) and acetoacetyl-CoA dehydrogenase (PhaB), exist in several natural PHA-producing microorganisms (Table 1) (Taroncher-Oldenburg et al., 2000).

While it is generally perceived that longer-chain 3-hydroxyacids are more biologically active than shorter-chain ones, their biosynthesis faces various technological and economic challenges that ultimately limit their industrial applications. In particular, 3-hydroxyvalerate (3-HV), a C5-counterpart of 3-HB, serves as a potential building block for the production of pharmaceuticals, such as renin inhibitors (Williams et al., 1991). It is also desirable to include 3-HV monomers into the PHB chain to form poly(3-hydroxybutyrate-*co*-3-hydroxyvalerate) (PHBV), a biocopolymer more ductile, flexible, and tougher than the PHB homopolymer (Lau et al., 2014; Snell and Peoples, 2009). Structurally, 3-HV can be derived based on a biosynthetic pathway similar to that of 3-HB (Figs. 1 and 2) except one acetyl-CoA precursor moiety is replaced with propionyl-CoA. However, propionyl-CoA is an uncommon metabolic intermediate for the vast majority of microorganisms. As a result, biosynthesis of 3-HV or 3-HV-containing biocopolymers requires supplementation of related, but often expensive, carbons such as propionate, valerate, 3-hydroxynitrile, and levulinate (Martin and Prather, 2009), significantly increasing the production cost. To date, only one metabolic study reported microbial production of 3-HV using unrelated carbon sources by extending the threonine biosynthetic pathway to form propionyl-CoA in bacterium *Escherichia coli* (Tseng et al., 2010).

Herein, we report an alternative approach to engineer *E. coli* strains for heterologous production of 3-HV from unrelated and cheap carbon sources. A previously derived propanologenic (i.e., 1-propanol-producing) *E. coli* strain with its genomic Sleeping beauty mutase (Sbm) operon being activated was used as the production host (Srirangan et al., 2013, 2014). The Sbm operon consists of four genes, i.e., *sbm-ygfD-ygfG-ygfH*, whose encoding enzymes are involved in extended dissimilation of succinate for fermentative production of 1-propanol or propionate with propionyl-CoA as a metabolic hub (Fig. 1) (Froese et al., 2009; Haller et al., 2000). Note that propionyl-CoA is a key precursor to 3-HV and does not normally exist in natural microorganisms. Biosynthesis of 3-HV involves three major enzymatic reactions (Fig. 2), i.e., (i) hetero-fusion of acetyl-CoA and propionyl-CoA molecules (i.e., Claisen condensation) via β-ketothiolase, generating 3-ketovaleryl-CoA, (ii) reduction of 3-ketovaleryl-CoA to chiral 3-hydroxyvaleryl-CoA (3-HV-CoA) by an enantiomer-specific dehydrogenase (ESD), and (iii) conversion of 3-HV-CoA to 3-HV via a CoA-removing enzyme. To enhance 3-HV production, we first targeted 3-hydroxyacid biosynthesis pathway by identifying and cloning relevant genes for functional expression. Then, we identified potential genetic, metabolic, and bioprocessing factors limiting 3-HV biosynthesis in *E. coli*. Finally, we developed metabolic engineering strategies by redirecting more carbon flux toward the Sbm pathway and various key *E. coli* host genes involved in the tricarboxylic acid (TCA) cycle were manipulated for the carbon flux redirection.

2. Materials and methods

2.1. Bacterial strains and plasmids

Bacterial strains, plasmids, and DNA primers used in this study are listed in Table S1. Genomic DNA from various bacterial strains was isolated using the Blood & Tissue DNA Isolation Kit (Qiagen, Hilden, Germany). Standard recombinant DNA technologies were applied for molecular cloning (Miller, 1992). All plasmids were constructed by Gibson enzymatic assembly (Gibson et al., 2009). Phusion HF and *Taq* DNA polymerases were obtained from New England Biolabs (Ipswich, MA, USA). All synthesized oligonucleotides were obtained from Integrated DNA Technologies (Coralville, IA, USA). DNA sequencing was conducted by the Centre for Applied Genomics at the Hospital for Sick Children (Toronto, Canada). *E. coli* BW25113 was the parental strain for derivation of all mutant strains in this study and *E. coli* DH5α was used as a host for molecular cloning. The *ldhA* gene (encoding lactate dehydrogenase) was inactivated in BW25113, generating BWΔ*ldhA*, with the intention of reducing lactate accumulation (Srirangan et al., 2014).

Activation of the genomic Sbm operon in BWΔ*ldhA* to generate propanologenic *E. coli* CPC-Sbm was described previously (Srirangan et al., 2014). Knockouts of the genes, including *glpK, glpD, glpABC, gldA, ptsI, dhaKLM*, *frdB*, *aceA, sucD*, *sdhA*, and *iclR* were introduced into CPC-Sbm by P1 phage transduction (Miller, 1992) using the appropriate Keio Collection strains (The Coli Genetic Stock Center, Yale University, New Haven, CT, USA) as donors (Baba et al., 2006). To eliminate the co-transduced FRT-Km^R-FRT cassette, the transductants were transformed with pCP20 (Cherepanov and Wackernagel, 1995), a temperature sensitive plasmid expressing a flippase (Flp) recombinase. Upon Flp-mediated excision of the Km^R cassette, a single Flp recognition site (FRT "scar site") was generated. Plasmid pCP20 was then removed by growing cells at 42 °C. The genotypes of derived knockout strains were confirmed by colony PCR using the appropriate verification primer sets listed in Table S1.

The *phaAB* operon was amplified by polymerase chain reaction (PCR) using the primer set g-phaAB and the genomic DNA of wild-type *Cupriavidus necator* ATCC 43291 as the template. The amplified operon was Gibson–assembled (Note that "assembled" is used for subsequent appearance) with the PCR-linearized pTrc99a using the primer set g-pTrc-phaAB to generate pTrc-PhaAB. All genes inserted into pTrc99a vector were under the control of the P_{trc} promoter. The DNA fragments *phaA* and *phaB* from pTrc-PhaAB were individually PCR-amplified using the primer sets g-phaA and g-phaB, and then assembled with the PCR-linearized pTrc99a using the corresponding primer sets (i.e., g-pTrc-phaA and g-pTrc-phaB), generating pTc-PhaA and pTrc-PhaB, respectively. Plasmid pK-BktB-Hbd-TesB was previously constructed in our lab by PCR-amplifying *bktB* from *C. necator* ATCC 43291, *hbd* from *Clostridium acetobutylicum* ATCC 824, and *tesB* from *E. coli* BW25141 using the corresponding primer sets (i.e., g-bktB, g-hbd, and g-tesB), followed by assembling all three PCR-amplified fragments with the PCR-linearized pK184 using the primer set g-pK-bktB-hbd-tesB. All genes inserted into pK184 vector were under the control of the P_{lac} promoter. To construct pK-TesB, the primer set g-tesB2 was used to

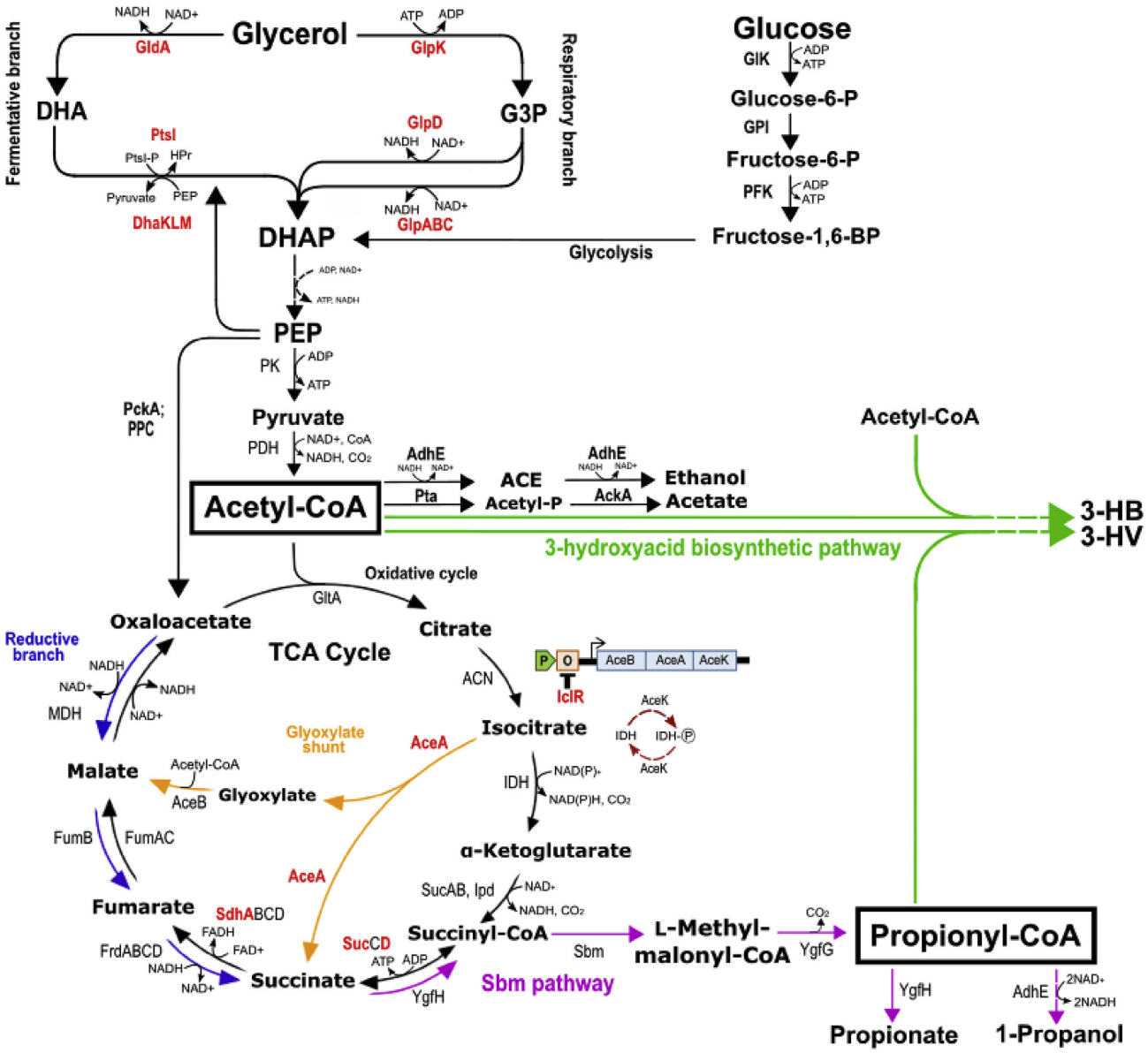

Fig. 1. Schematic representation of natural and engineered pathways in *E. coli* using glucose or glycerol as the carbon source. Proteins targeted for mutation are in red. Metabolic pathways outlined: glycolysis, TCA cycle, fermentative/respiratory branch of glycerol utilization pathway (in black); engineered 3-hydroxyacid pathways (in green); engineered Sleeping beauty mutase pathway (in purple). Metabolite abbreviations: 3-HB, 3-hydroxybutyrate; 3-HV, 3-hydroxyvalerate; ACE, acetaldehyde; Acetyl-P, acetyl-phosphate; DHA, dihydroxyacetone; DHAP, dihydroxyacetone phosphate; Fructose-1,6-BP, fructose-1,6-bisphosphate; Fructose-6-P; fructose-6-phosphate; G3P, glycerol-3-phosphate; Glucose-6-P; glucose-6-phosphate; PEP, phosphoenolpyruvate. Protein abbreviations: AceA, isocitrate lyase; AceB, malate synthase A; AceK, isocitrate dehydrogenase kinase/phosphatase; AckA, acetate kinase; AdhE, aldehyde-alcohol dehydrogenase; ACN, aconitase; DhaKLM, dihydroxyacetone kinase; FrdABCD, fumarate reductase complex; FumA, fumarate hydratase class I (aerobic); FumB, fumarate hydratase class I (anaerobic); FumC, fumarate hydratase class II; GldA, glycerol dehydrogenase; GlK, glucose kinase; GlpABC, anaerobic glycerol-3-phosphate dehydrogenase; GlpD, aerobic glycerol-3-phosphate dehydrogenase; GlpK, glycerol kinase; GltA, citrate synthase; GPI, glucose-6-phosphate isomerase; Hpr, phosphocarrier protein; ICD, isocitrate dehydrogenase; IclR, AceBAK operon repressor; IDH, isocitrate dehydrogenase; IDH-P, isocitrate dehydrogenase-phosphate; Ipd, lipoamide dehydrogenase; MDH, malate dehydrogenase; PckA, phosphoenolpyruvate carboxykinase; PDH, pyruvate dehydrogenase; PFK, phosphofructokinase; PFL, pyruvate formate lyase; PK, pyruvate kinase; PPC, phosphoenolpyruvate carboxylase; Pta, phosphotransacetylase; PtsI, PTS enzyme I; Sbm, methylmalonyl-CoA mutase; SdhABCD, succinate dehydrogenase complex; SucAB, 2-oxoglutarate dehydrogenase; SucCD, succinyl coenzyme A synthetase; YgfG, (*R*)-methyl-malonyl-CoA carboxylase; YgfH, propionyl-CoA: succinate CoA-transferase. (For interpretation of the references to colour in this figure legend, the reader is referred to the Web version of this article.)

PCR-amplify *tesB* from pK-BktB-Hbd-TesB and the amplicon was subsequently assembled with the PCR-linearized pK184 using the primer set g-pK-tesB. The two-subunit β-ketothiolase gene *bktBαβ* was PCR-amplified from the genomic DNA of wild-type *Haloferax mediterranei* ATCC 33500 using the primer set g-bktBαβ. The amplicon was then assembled with the PCR-linearized pK-TesB using the primer set g-pK-bktαβ-tesB, yielding pK-BktBαβ-TesB. The same approach was used with the primer set g-pK-bktB-tesB to generate plasmid pK-BktB-TesB harboring the *bktB* gene. Plasmid pK-BktB-Hbd was constructed by PCR-amplifying *hbd* from pK184-BktB-Hbd-TesB using the primer set g-pK-bktB-hbd, followed by assembling the amplicon with the PCR-linearized pK-BktB using the primer set g-pK-bktB. Lastly, to generate plasmids testing CoA removing efficiency (i.e., pK-BktB-Hbd-Ptb-Buk and pK-BktB-Hbd-Pct), the *ptb-buk* operon from *C. acetobutylicum* ATCC 824 and *pct* from *Clostridium propionicum* DSM 1682 were PCR amplified using corresponding primer sets (i.e., g-ptb-buk and g-pct). The *ptb-buk*

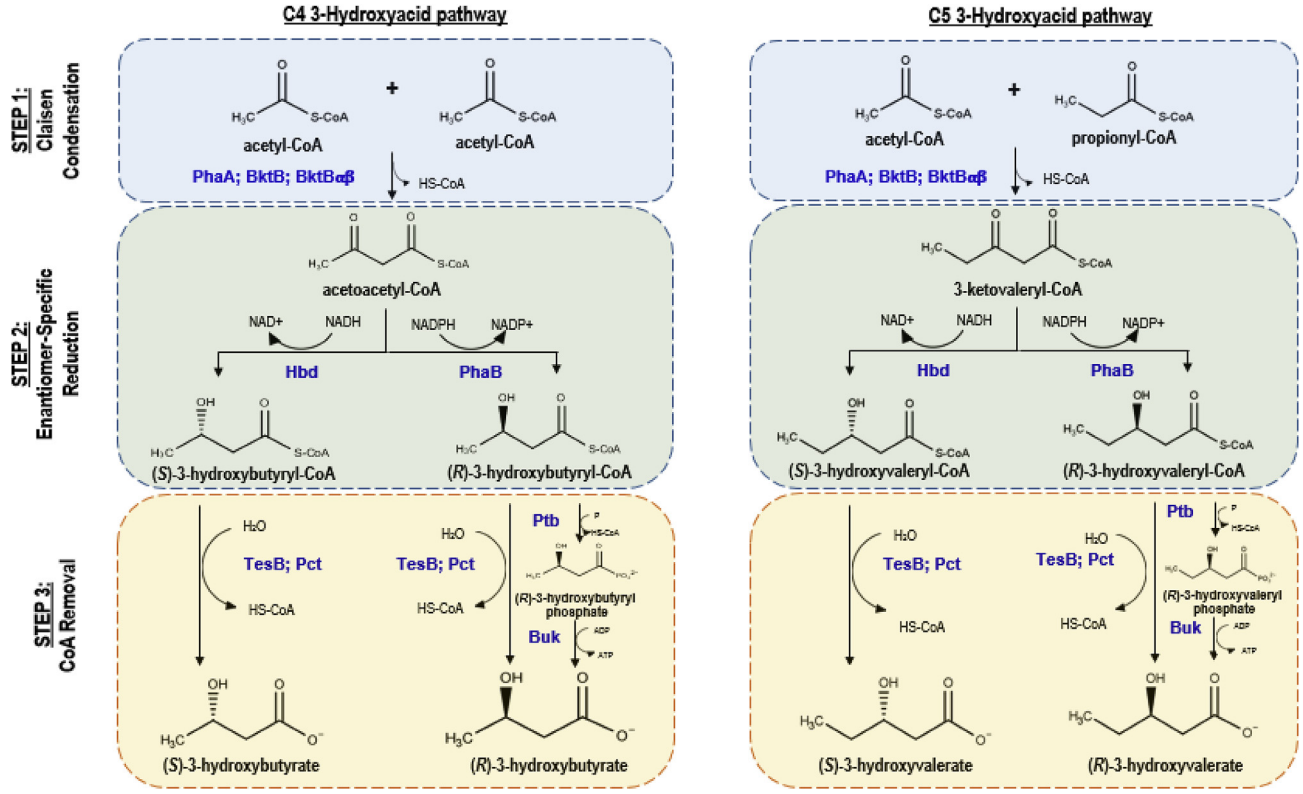

Fig. 2. Schematic representation of engineered three-step 3-hydroxyacid pathways. Origin and function of enzymes involved in the 3-hydroxyacid producing pathways can be found in Table 1. Protein abbreviations: BktB, beta-ketothiolase; BktBαβ, PHA-specific beta-ketothiolase – alpha and beta subunits; Buk, butyrate kinase; Hbd, beta-hydroxybutyryl-CoA dehydrogenase; Pct, acetate/propionate CoA-transferase; PhaA, acetoacetyl-CoA thiolase; PhaB, acetoacetyl-CoA dehydrogenase; Ptb, phosphotransbutyrylase; TesB, acyl-CoA thioesterase II.

and *pct* amplicons were then individually assembled with PCR linearized pK-BktB-Hbd using g-pK-bktB-hbd-ptb-buk and g-pK-bktB-hbd-pct primer sets, respectively.

2.2. Bacterial cultivation

All medium components were obtained from Sigma-Aldrich Co. (St Louis, MO, USA) except glucose, yeast extract, and tryptone which were obtained from BD Diagnostic Systems (Franklin Lakes, NJ, USA). The media were supplemented with antibiotics as required: 25 $\mu g\,ml^{-1}$ kanamycin and 50 $\mu g\,ml^{-1}$ ampicillin. *E. coli* strains, stored as glycerol stocks at −80 °C, were streaked on LB agar plates with appropriate antibiotics and incubated at 37 °C for 14–16 h. Single colonies were picked from LB plates to inoculate 30-ml LB medium (10 $g\,l^{-1}$ tryptone, 5 $g\,l^{-1}$ yeast extract, and 5 $g\,l^{-1}$ NaCl) with appropriate antibiotics in 125-ml conical flasks. The cultures were shaken at 37 °C and 280 rpm in a rotary shaker (New Brunswick Scientific, NJ, USA) and used as seed cultures to inoculate 220 ml LB media at 1% (v/v) with appropriate antibiotics in 1-L conical flasks. This second seed culture was shaken at 37 °C and 280 rpm until an optical density of 0.80 OD_{600} was reached. Cells were then harvested by centrifugation at 9000 ×g and 20 °C for 10 min and resuspended in 30-ml modified M9 production media. The suspended culture was transferred into a 125-ml screw-cap or vent-cap plastic production flasks and incubated at either 30 or 37 °C at 280 rpm in a rotary shaker. Unless otherwise specified, the modified M9 production medium contained 30 $g\,l^{-1}$ glycerol or glucose, 2.5 $g\,l^{-1}$ succinate, 5 $g\,l^{-1}$ yeast extract, 10 mM $NaHCO_3$, 1 mM $MgCl_2$, 0.2 µM cyanocobalamin (vitamin B12), 5th dilution of M9 salts mix (33.9 $g\,l^{-1}$ Na_2HPO_4, 15 $g\,l^{-1}$ KH_2PO_4, 5 $g\,l^{-1}$ NH_4Cl, 2.5 $g\,l^{-1}$ NaCl), $1{,}000^{th}$ dilution of Trace Metal Mix A5 (2.86 $g\,l^{-1}$ H_3BO_3, 1.81 $g\,l^{-1}$ $MnCl_2{\cdot}4H_2O$, 0.222 $g\,l^{-1}$ $ZnSO_4{\cdot}7H_2O$, 0.39 $g\,l^{-1}$ $Na_2MoO_4{\cdot}2H_2O$, 79 $\mu g\,l^{-1}$ $CuSO_4{\cdot}5H_2O$, 49.4 $\mu g\,l^{-1}$ $Co(NO_3)_2{\cdot}6H_2O$), and supplemented with 0.1 mM isopropyl β-D-1-thiogalactopyranoside (IPTG). All cultivation experiments were performed in triplicate.

2.3. Analytical methods

Culture samples were appropriately diluted with 0.15 M saline solution for measuring the optical cell density (OD_{600}) using a spectrophotometer (DU520, Beckman Coulter, Fullerton, CA). Cell-free medium was collected by centrifugation of the culture sample at 9000 ×g and filter sterilized for titer analysis of glucose or glycerol, and various metabolites using a high-performance liquid chromatography (HPLC; LC-10AT, Shimadzu, Kyoto, Japan) with a refractive index detector (RID; RID-10A, Shimadzu, Kyoto, Japan) and a chromatographic column (Aminex HPX-87H, Bio-Rad Laboratories, CA, USA). The HPLC column temperature was maintained at 35 °C and the mobile phase was 5 mM H_2SO_4 (pH 2.0) running at 0.6 ml min^{-1}. The RID signal was acquired and processed by a data processing unit (Clarity Lite, DataApex, Prague, Czech Republic).

3. Results

3.1. Pathway implementation for heterologous 3-HV biosynthesis

An essential precursor for 3-HV biosynthesis is propionyl-CoA, which is non-native to *E. coli*. By activating the Sbm operon in the *E. coli* host genome, the dissimilation of succinate can be diverted from the TCA cycle into the Sbm pathway to form propionyl-CoA (Fig. 1). To evaluate the feasibility of 3-HV biosynthesis using this propanologenic host strain, a double plasmid system was employed in strain P3HA11 (Fig. 3). In the first step, hetero-fusion of propionyl-CoA and acetyl-CoA to 3-ketovaleryl-CoA was carried out by PhaA (encoded by *phaA*) (Fig. 2). Subsequently in the second step, the enantiomer-specific

Table 1
List of relative enzymes, their origin, and enzymatic functions in 3-hydroxyacid biosynthetic pathway.

3-HA pathway	Enzyme(s)	Gene(s) (locus_tag)[a]	Source organism	Function(s)
				3-HB production 3-HV production
Step 1: Claisen condensation	Acetoacetyl-CoA thiolase	*phaA* (H16_RS07140)	*Cupriavidus necator* ATCC 43291	Homofusion of 2 acetyl-CoA moieties
	β-ketothiolase	*bktB* (H16_A1445)	*Cupriavidus necator* ATCC 43291	Homofusion of 2 acetyl-CoA moieties
	PHA-specific beta-ketothiolase alpha and beta subunits	*bktBα* (HFX_6004), *bktBβ* (*HFX_6003*)	*Haloferax mediterranei* ATCC 33500	Homofusion of 2 acetyl-CoA moieties
Step 2: Enantiomer-specific reduction (ESR)	Acetoacetyl-CoA reductase ((*R*)-3HB-CoA dehydrogenase)+	*phaB* (H16_A1439)	*Cupriavidus necator* ATCC 43291	Reduction of acetoacetyl-CoA to (*R*)-3-HB-CoA
	β-hydroxybutyryl-CoA dehydrogenase ((*S*)–3HB-CoA dehydrogenase)	*hbd* (CA_C2708)	*Clostridium acetobutylicum* ATCC 824	Reduction of acetoacetyl-CoA to (*S*)–3-HB-CoA
Step 3: CoA removal	Acyl-CoA thioesterase II	*tesB* (AW869_16290)	*Escherichia coli* BW25141	Hydrolysis of (*S*) and (*R*)-3-HB-CoA to racemic 3-HB
	Phosphate butyryltransferase, Butyrate kinase	*ptb* (CA_C3076), *buk* (CA_C3075)	*Clostridium acetobutylicum* ATCC 824	Catalyze the conversion of (*R*)-3-HB-CoA to (*R*)-3-HB-P, dephosphorylation to (*R*)-3-HB
	Acetate/propionate CoA-transferase	*pct* (CPRO_08400)	*Clostridium propionicum* DSM 1682	Removes CoA moieties to generate racemic 3-HB (reversible reaction)

[a] Gene locus tags were obtained from the National Center for Biotechnology Information (NCBI) GenBank nucleotide database.

reduction (ESR) of 3-ketovaleryl-CoA into (*R*)-3-HV-CoA is catalyzed by NADPH-dependent PhaB (encoded by *phaB*). In the final step, (*R*)-3-HV is synthesized via hydrolysis of (*R*)-3-HV-CoA, catalyzed by acyl-CoA thioesterase II (i.e., TesB encoded by *tesB*). Note that these (*R*)-3-HV-producing enzymes also have the capacity to generate the C4 counterparts in all steps of the engineered pathway, resulting in the co-production of 3-HV and 3-HB (Fig. 2). To validate the proposed 3-hydroxyacid pathway, P3HA11 was cultivated in a 37 °C shake-flask using 30 g l^{-1} glucose (Fig. 3), producing 0.27 g l^{-1} 3-HB and 0.03 g l^{-1} 3-HV. On the other hand, the control strain CPC-Sbm without the 3-hydroxyacid biosynthetic pathway produced no 3-hydroxyacids, indicating that the implemented pathway was functional. Also, the loss of either one of the 3-hydroxyacid pathway genes resulted in no 3-HV production (see later sections and Fig. 4), suggesting that all these 3-hydroxyacid biosynthetic pathway genes were required for 3-HV production. Furthermore, another control strain BWΔ*ldhA*-3HA11 with the native (i.e., non-activated) Sbm operon produced 0.94 g l^{-1} 3-HB but no 3-HV, suggesting that propionyl-CoA acted as a key precursor for 3-HV biosynthesis.

3.2. Manipulation of genes involved in 3-HV biosynthetic pathway

As multiple enzymes have been identified to catalyze each of the three steps in the 3-HV biosynthetic pathway (Table 1), the effects of heterologous expression of these enzyme genes, either individually or in combination, on 3-HV production were investigated. For the first step of Claisen condensation, in addition to PhaA which primarily targets short-chain CoA molecules, BktB (encoded by *bktB*) is another β-ketothiolase with a specificity toward long-chain CoA molecules (Slater et al., 1998). While the control strain P3HA10 produced no 3-hydroxyacids, heterologous expression of either *phaA* in P3HA11 or *bktB* in P3HA12 mediated both 3-HV and 3-HB production (Fig. 4), suggesting the catalytic activity of the two β-ketothiolases for the Claisen condensation. Heterologous expression of another PHA-specific β-ketothiolase (i.e., BktBαβ encoded by *bktBαβ*) in P3HA13 mediated the production of 3-HB only, but not 3-HV. Note that BktB appeared to be more effective than PhaA in terms of 3-HV production, potentially due to the promiscuous activity of BktB toward different acyl-CoA moieties (Slater et al., 1998). Interestingly, compared to P3HA11 and P3HA12, coexpression of both β-ketothiolase genes of *bktB* and *phaA* in P3HA21 significantly enhanced 3-hydroxacid production up to 0.77 g l^{-1} 3-HB and 0.11 g l^{-1} 3-HV. Due to this synergistic effect, the engineered strains used in all subsequent experiments contained both *bktB* and *phaA* genes.

For the second step of ESR, in addition to PhaB, we also evaluated another NADH-dependent dehydrogenase, i.e., β-hydroxybutyryl-CoA dehydrogenase (also known as (*S*)-3-HB-CoA dehydrogenase or Hbd encoded by *hbd*) and their effects on 3-HV production are summarized in Fig. 4. PhaB and Hbd mediate the formation of (*R*)- and (*S*)-form hydroxyacid-CoA, respectively (Fig. 2). The control strain P3HA20 without a heterologous dehydrogenase produced no 3-HV though a trace amount of 3-HB at 0.08 g l^{-1} was observed, presumably associated with non-specific dehydrogenases in *E. coli*. The overall synthesis of (*R*)-3-HB/HV from PhaB in P3HA21 was approximately 3-fold that of (*S*)-3-HB/HV from Hbd in P3HA22. Coexpression of *phaB* and *hbd* further improved the production of 3-hydroxyacids and, interestingly, the total 3-hydroxyacid titers of P3HA31 (1.07 g l^{-1} 3-HB and 0.19 g l^{-1} 3-HV) were approximately equivalent to the sum of the 3-hydroxyacid titers of P3HA21 (0.77 g l^{-1} 3-HB and 0.11 g l^{-1} 3-HV) and P3HA22 (0.24 g l^{-1} 3-HB and 0.04 g l^{-1} 3-HV), implying the potentially independent enzymatic mechanisms for the two dehydrogenases. Due to the improved 3-HV production in P3HA31, this dehydrogenase duo was used in all subsequent experiments.

For the last step, in addition to the native TesB, we also evaluated two other CoA-removing enzymes, including phosphotransbutyrylase (i.e., Ptb encoded by *ptb*) and butyrate kinase (i.e., Buk encoded by *buk*)

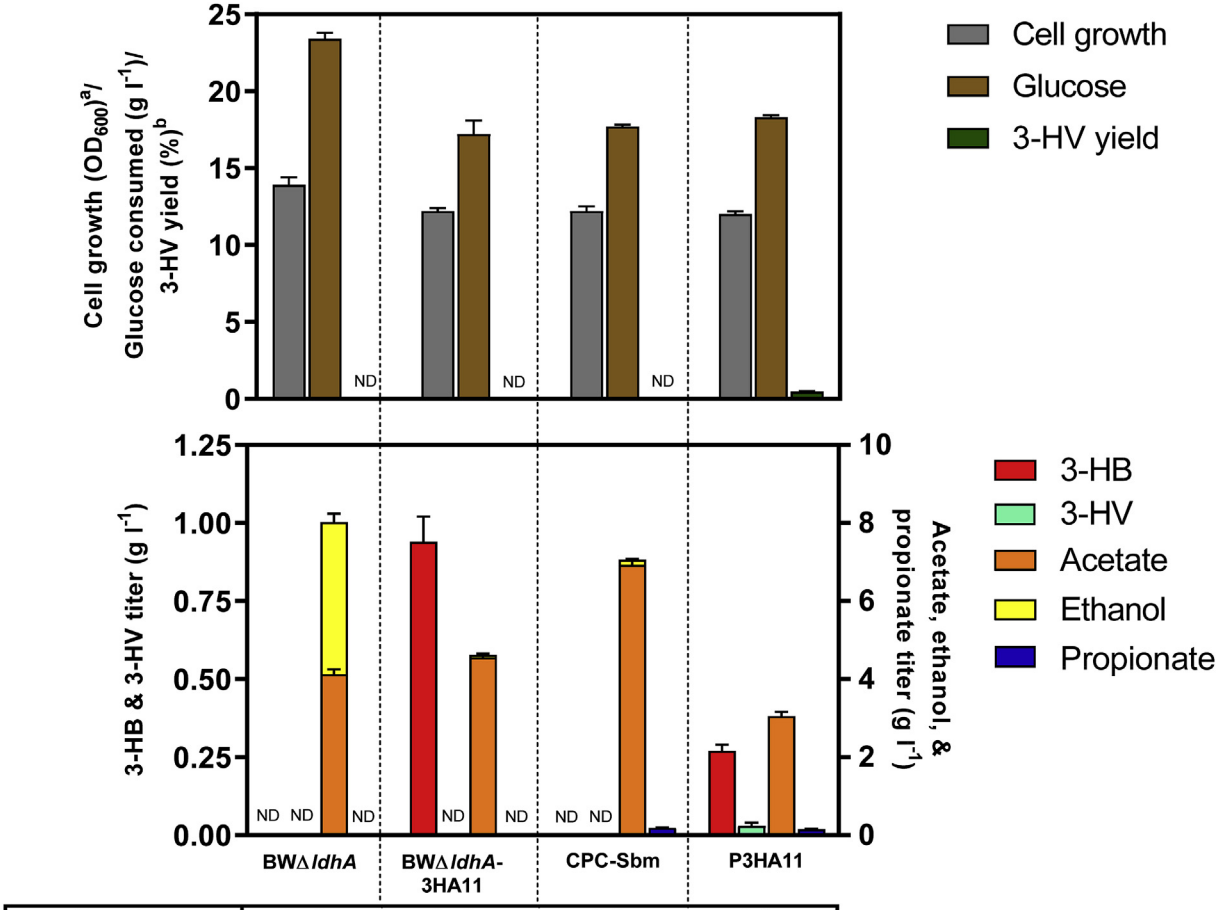

Sbm pathway	Inactive	Inactive	Active	Active
3-HA pathway steps				
1. Claisen condensation	n/a	PhaA	n/a	PhaA
2. ESR	n/a	PhaB	n/a	PhaB
3. CoA removing enzyme	n/a	TesB	n/a	TesB

[a] Measured cell density after 48h cultivation using spectrophotometer (OD_{600}), time 0h cell density was kept at ~5.00
[b] Defined as the percentage of the 3-HV theoretical yield based on the consumed glucose
3-HA 3-hydroxyacid
ESR enantiomer specific reduction
n/a not applicable
ND not detected

Fig. 3. Construction of 3-HV-producing strain from unrelated carbon source by engineering Sbm and 3-hydroxyacid biosynthetic pathways. Strains compared are BWΔ*ldhA*, BWΔ*ldhA*-3HA11, CPC-Sbm, and P3HA11. Top panel represents cell growth (OD_{600}), glucose consumption, and 3-HV yield (%) while bottom panel represents titers of 3-HB, 3-HV, even/odd-chain acids (i.e., acetate and propionate), and ethanol reached after 48h shake-flask cultivation. All values are reported as means ± SD (n = 3).

and acetate/propionate CoA-transferase (i.e., Pct encoded by *pct*), and their effects on 3-HV production are summarized in Fig. 4. The Ptb-Buk system is a two-step CoA removal scheme generating a phosphorylated intermediate and has been successfully used for butyrate and 3-HB production (Fischer et al., 2010; Gao et al., 2002). On the other hand, Pct has a broad substrate specificity toward CoA molecules and is capable of converting both (*R*) and (*S*) forms of 3-HB-CoA into respective 3-HB (Matsumoto et al., 2013). The control strain P3HA30 without a CoA-removing enzyme produced no 3-hydroxyacids. In comparison to P3HA31, expression of *ptb-buk* in P3HA32 or *pct* in P3HA33 did not further improve 3-HV biosynthesis. Given the superior CoA removing nature of TesB in comparison to Ptb-Buk and Pct, we chose not to conduct further enzyme co-expression for this step and thus only TesB was used for CoA removal in all subsequent experiments.

3.3. Bacterial cultivation for 3-HV production

As the metabolic activities of various pathways involved for 3-HV biosynthesis (Fig. 1) can potentially depend on culture environment, we examined the effects of cultivation conditions, specifically temperature and carbon source (Fig. 5), on 3-HV production. While the formation of propionyl-CoA in the fermentative Sbm pathway is favored by anaerobic conditions (Akawi et al., 2015; Srirangan et al., 2014), the hydroxyacid biosynthetic pathway is energetically intensive and presumably favored by aerobic conditions. However, precise control of the oxygenic condition for shaker flask cultivation was difficult though the shaking speed could be adjusted. For consistent operation in this study, the shaking speed was fixed to 280 rpm throughout the entire cultivation. Under both 30 °C and 37 °C, the control strain CPC-Sbm lacking a 3-hydroxyacid biosynthetic pathway produced neither 3-HB nor 3-HV (Table S6). However, the overall yield of odd-chain metabolites, including 3-HV, propionate, and 1-propanol, based on the consumed

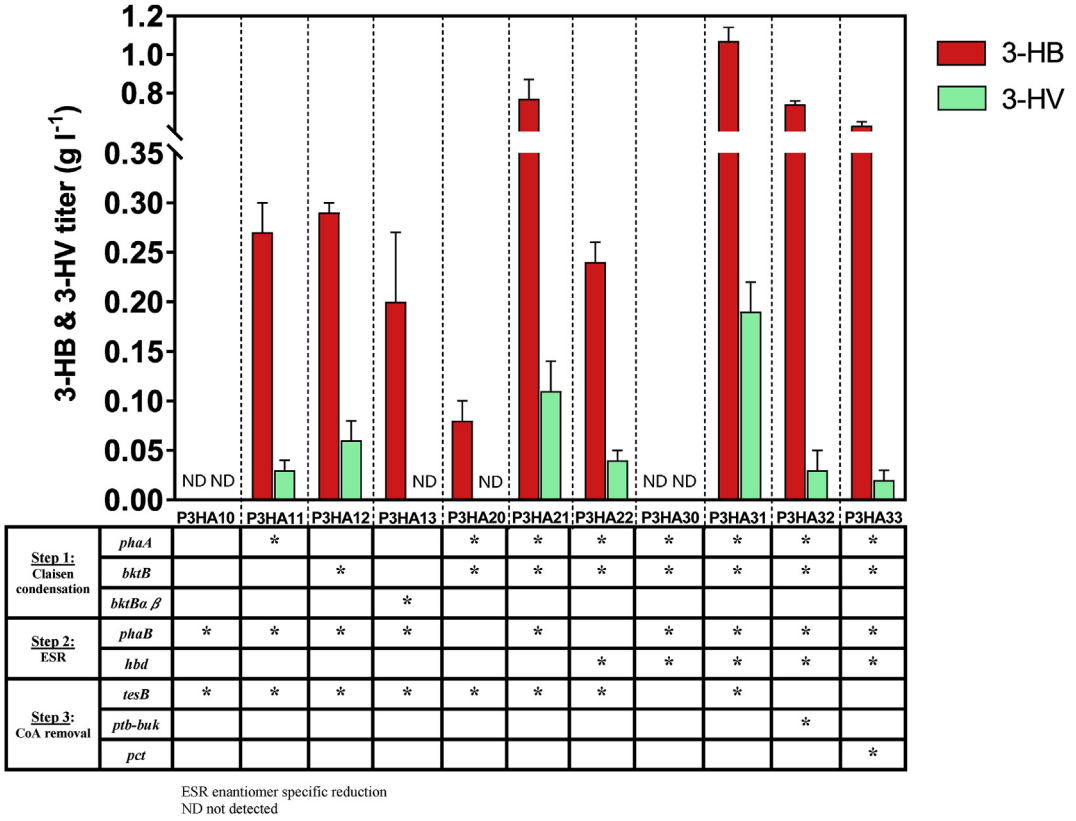

Fig. 4. Modular construction of 3-HV biosynthetic pathway by establishing efficient Claisen condensation, reduction reaction, and CoA removing capabilities. Strains compared are P3HA10, P3HA11, P3HA12, P3HA13, P3HA20, P3HA21, P3HA22, P3HA30, P3HA31, P3HA32, and P3HA33. Panel represents titers of 3-HB and 3-HV. Cells labeled with an asterisk represent overexpressed genes. All values are reported as means ± SD (n = 3).

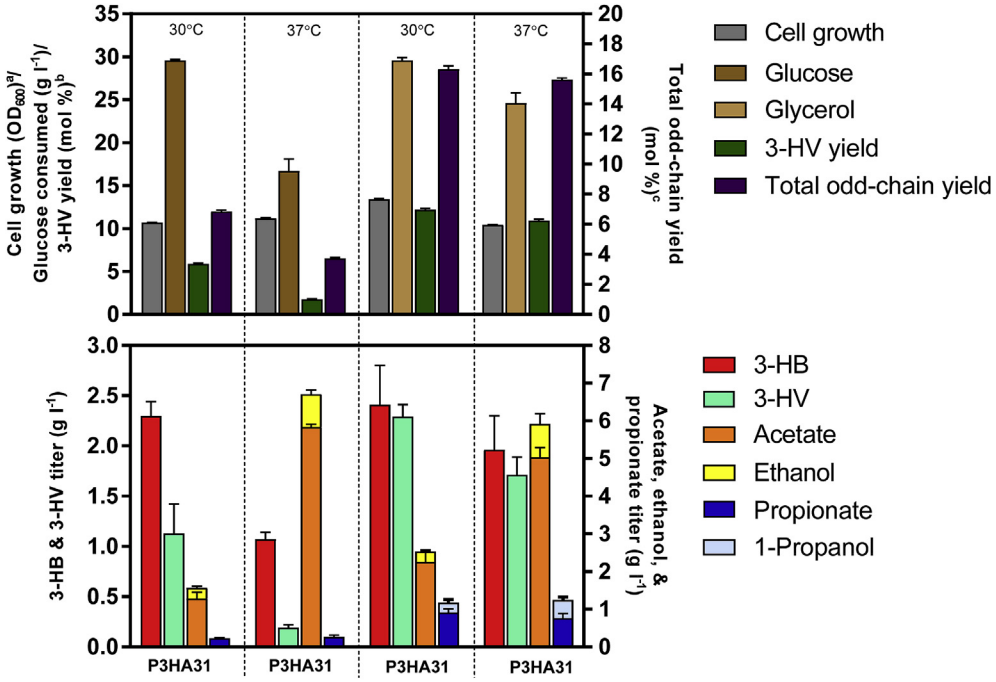

[a] Measured cell density after 48h cultivation using spectrophotometer (OD_{600}), time 0h cell density was kept at ~5.00
[b] Defined as the percentage of the 3-HV theoretical yield based on the consumed glucose
[c] Defined as the percentage of the total odd-chain metabolites (i.e., propionate, 1-propanol, and 3-HV) theoretical yield based on the consumed glucose/glycerol

Fig. 5. Effects of cultivation temperature and carbon source on 3-HV production in P3HA31. Top panel represents cell growth (OD_{600}), glucose/glycerol consumption, 3-HV yield (%), and total odd-chain (i.e., 3-HV, propionate, and 1-propanol) yield (%) while bottom panel represents titers of 3-HB, 3-HV, even/odd-chain acids (i.e., acetate and propionate), and ethanol reached after 48h shake-flask cultivation. All values are reported as means ± SD (n = 3).

glucose was significantly higher under a low temperature, i.e., 4.42% under 30 °C vs. 1.34% under 37 °C. Note that the overall yield of odd-chain metabolites potentially correlates with the level of intracellular propionyl-CoA during cultivation. For P3HA31 with an optimal 3-hydroxyacid biosynthetic pathway, both 3-HB and 3-HV titers of the 30 °C culture were significantly higher than those of the 37 °C culture. In addition, the overall yield of odd-chain metabolites based on the consumed glucose was favored by a low cultivation temperature, i.e., 6.84% under 30 °C vs. 3.74% under 37 °C. Notably, for both strains, the low cultivation temperature under 30 °C appeared to significantly reduce carbon spill toward acetate and ethanol, therefore enhancing the metabolic availability of acetyl-CoA for 3-hydroxyacid production. Furthermore, the overall glucose consumption and cell growth were also more effective under a low temperature of 30 °C.

Given the abundance as a byproduct of biodiesel production, glycerol has become a promising feedstock for bio-based production (Gonzalez et al., 2008; Yazdani and Gonzalez, 2007). Since glycerol possesses a high degree of reductance ($\kappa = 4.67$), its glycolytic degradation generates approximately twice the number of reducing equivalents compared to xylose and glucose ($\kappa = 4.00$) (Murarka et al., 2008). Cultivation of P3HA31 with glycerol at 30 °C resulted in a high 3-HV titer of 2.29 g l^{-1}, which is approximately 2-fold that of the corresponding glucose culture. Similarly, cultivation of P3HA31 with glycerol at 37 °C resulted in a 3-HV titer of 1.71 g l^{-1}, which is approximately 9-fold that of the corresponding glucose culture, further confirming both the temperature and carbon source effects on 3-HV production. Importantly, the overall yield of odd-chain metabolites was elevated with glycerol as the carbon source, i.e., 16.31% under 30 °C and 15.63% under 37 °C. These results are consistent with our previous reports that glycerol is a more efficient carbon source in stimulating the Sbm pathway (Akawi et al., 2015; Srirangan et al., 2016). Hence, cultivation with glycerol as the sole carbon source under 30 °C was adopted for all subsequent experiments.

3.4. Metabolic engineering to enhance 3-HV production

Propionyl-CoA, a key precursor for 3-HV biosynthesis, is derived via a partial carbon flux diversion of the TCA cycle at the node of succinyl-CoA into the Sbm pathway (Fig. 1). To enhance 3-HV biosynthesis, we developed various metabolic strategies by manipulating a selection of TCA genes to increase such carbon flux redirection and the results are summarized in Fig. 6. We first supplemented the culture of P3HA31 with succinate and observed that propionate and 3-HV titers were increased upon succinate supplementation, suggesting that the carbon flux redirection into the Sbm pathway could be limited by succinate availability. We then targeted several TCA genes encoding enzymes near the succinate note (designated in red in Fig. 1) for manipulation. Consequently, we derived various mutants by individually blocking the three major TCA routes, i.e. oxidative TCA cycle, reductive TCA branch, and glyoxylate shunt. Compared to the control strain P3HA31, inactivation of the reductive TCA branch gene of *frdB* in P3HA31Δ*frdB* significantly reduced 3-HV titer and yield, whereas 3-HV production was slightly reduced upon the inactivation of the glyoxylate shunt gene of *aceA* in P3HA31Δ*aceA* or the oxidative TCA cycle gene of *sdhA* in P3HA31Δ*sdhA*. The results suggest that the carbon flux redirected toward the Sbm pathway was primarily derived from the reductive TCA branch. Simultaneous inactivation of the reductive TCA branch and glyoxylate shunt in the double mutant P3HA31Δ*frdB*Δ*aceA* further reduced 3-HV production with an 8-fold reduction in the total odd-chain yield compared to the control P3HA31, further suggesting a minimal contribution from the oxidative TCA cycle for the carbon flux redirection. Importantly, disruption of *sucD* caused a complete abolishment in biosynthesis of all odd-chain metabolites, including 3-HV, 1-propanol, and propionate, suggesting the key role that this succinate-succinyl-CoA interconversion step played for the carbon flux redirection into the Sbm pathway. Given that succinate appears to be critically limiting the carbon flux redirection, glyoxylate shunt was deregulated by mutating *iclR* in P3HA31Δ*iclR* to enlarge the succinate pool. P3HA31Δ*iclR* secreted a trace amount of succinate though 3-HV production was not improved compared to the control strain P3HA31. Note that these TCA-gene mutations appeared to minimally affect metabolic activity of the 3-hydroxyacid biosynthetic pathway since, compared to the control strain P3HA31, 3-HB titer and yield were slightly increased by all single mutations (ranging from 2.41 g l^{-1} to 2.76 g l^{-1} and from 14.6% to 19.8%, respectively) except Δ*sdhA* (which slightly reduced 3-HB titer and yield). As a potential reason limiting 3-HV production in P3HA31Δ*iclR* was the carbon flux diversion (toward both oxidative and reductive TCA directions) at the succinate node, we further blocked the oxidative TCA cycle by deriving a double mutant P3HA31Δ*sdhA*Δ*iclR* such that the entire carbon flux would be redirected into the Sbm pathway via the reductive TCA branch. While 3-hydroxyacid titers for this particular double mutant were increased moderately compared to the control strain P3HA31 (23.7% for 3-HB and 27.9% for 3-HV), the corresponding yields were increased significantly (~100% for both 3-HB and 3-HV), suggesting a much higher 3-hydroxyacid producing capacity and successful carbon flux redirection into the Sbm pathway under this genetic background. However, the culture performance was limited by deteriorated glycerol dissimilation and cell growth for P3HA31Δ*sdhA*Δ*iclR* cultivated in the standard screw-cap shake-flasks, which were rather anaerobic. Such limitation was partially resolved by conducting the same cultivation under a more aerobic condition in the vent-cap shake-flasks, resulting in the highest titers for both 3-HV (3.71 g l^{-1}) and propionate (2.97 g l^{-1}), a nearly 150% increase in the odd-chain yield compared to the control strain P3HA31 in the standard screw-cap shake-flasks.

4. Discussion

Among the three steps in the 3-hydroxyacid biosynthetic pathway, the Claisen condensation, generating acetoacetyl-CoA and 3-ketovaleryl-CoA, has to confront a thermodynamic hurdle caused by an energetically unfavorable fusion of two acyl-CoA molecules (Weber, 1991), and therefore can represent a rate-limiting step. While three individual β-ketothiolases of PhaA, BktB, and BktBαβ mediated homofusion of acetyl-CoA for 3-HB production, only PhaA and BktB mediated heterofusion of acetyl-CoA and propionyl-CoA for 3-HV production. BktB appeared to have a higher specificity than PhaA toward propionyl-CoA. Also, the catalytic effects of PhaA and BktB appeared to be synergistic when the two enzymes were coexpressed. Nevertheless, both PhaA and BktB had a significantly higher specificity toward acetyl-CoA than propionyl-CoA, limiting the 3-HV yield.

PhaB and Hbd mediate ESR of the 3-hydroxyacid biosynthetic pathway, generating (*R*)-3-HB/HV-CoA and (*S*)-3-HB/HV-CoA, respectively, and our results suggest that PhaB was catalytically more active than Hbd. In addition, the catalytic effects of PhaB and Hbd appeared to be independent and addable upon coexpression of the two enzymes. Since PhaB and Hbd are NADPH-dependent and NADH-dependent, respectively, our results of higher titers in (*R*)-3-HB/HV than (*S*)-3-HB/HV might imply the physiological abundance of NADPH as a reducing equivalent under the shake-flask culture conditions. Cofactor engineering has been applied to manipulate the physiological levels of reducing equivalents to improve the biosynthesis of an enantiomerically pure 3-hydroxyacid (Perez-Zabaleta et al., 2016).

Among the three evaluated CoA removing enzymes, the native TesB thioesterase outperformed Ptb-Buk and Pct in both 3-HB and 3-HV production. Consistent to our results, TesB is capable of catalyzing an irreversible one-step CoA removal hydrolysis and has a broad substrate specificity (Zheng et al., 2004). Note that the control strain P3HA30 produced no 3-hydroxyacids, suggesting that the expression of the native genomic *tesB* gene was insufficient or even inhibited. The low 3-hydroxyacid titers for P3HA32 might be associated with the limited substrate specificity toward (*R*)-3-hydroxyacid-CoA only. A previous

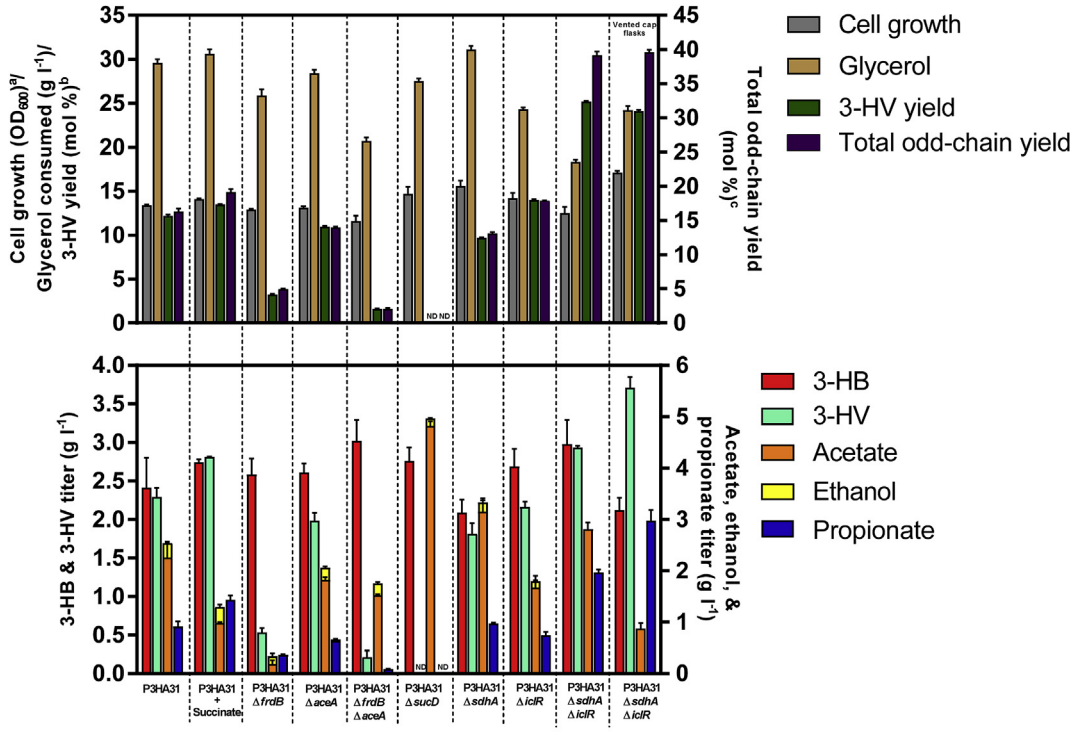

[a] Measured cell density after 48h cultivation using spectrophotometer (OD_{600}), time 0h cell density was kept at ~5.00
[b] Defined as the percentage of the 3-HV theoretical yield based on the consumed glycerol/succinate
[c] Defined as the percentage of the total odd-chain metabolites (i.e., propionate and 3-HV) theoretical yield based on the consumed
ND not detected

Fig. 6. Consolidating genetic and bioprocessing strategies for enhanced carbon flux toward succinate in TCA cycle. Top panel represents cell growth (OD_{600}), glycerol consumption, 3-HV yield (%), and total odd-chain (i.e., 3-HV, and propionate) yield (%) while bottom panel represents titers of 3-HB, 3-HV, even/odd-chain acids (i.e., acetate and propionate), and ethanol reached after 48h shake-flask cultivation. All values are reported as means ± SD (n = 3).

study reported that strains expressing Ptb-Buk yielded no (*S*)-3-HB (Tseng et al., 2009). While, similar to TesB, Pct also has a specificity toward both (*R*)- and (*S*)-3-hydroxyacid-CoA (Matsumoto et al., 2013), its catalytic activity was less effective than TesB based on our results. Note that, in order to alleviate the competition from the 3-HB biosynthetic pathway for enhanced 3-HV biosynthesis, protein engineering techniques to improve enzymatic specificity of β-ketothiolases toward odd-chain substrates could be potentially useful, as was successfully demonstrated for other proteins (Arabolaza et al., 2010; Sofeo et al., 2019). To the best of our knowledge, there are no reports demonstrating higher enzymatic preference for odd-chain precursors associated with the last two 3-HV reaction steps (i.e., reduction and CoA removal).

Culture conditions critically affected 3-HV production. The positive effects of the lower cultivation temperature were presumably associated with increased levels of intracellular propionyl-CoA. The temperature change could potentially affect the metabolic activity of the Sbm pathway. On the other hand, the specific 3-HB yields based on consumed glycerol were approximately the same under both 30 °C and 37 °C (Fig. 5), suggesting that the metabolic activity of the 3-hydroxyacid biosynthetic pathway was minimally affected by temperature. Previously, glycerol was shown to outperform glucose as the carbon source in terms of stimulating the metabolic activity of the Sbm pathway in propanologenic *E. coli* strains (Akawi et al., 2015; Srirangan et al., 2014). Such observation was further demonstrated in the current study. The higher reductance of glycerol than glucose could generate more reducing equivalents for their subsequent use in the 3-hydroxyacid biosynthetic pathway.

In *E. coli*, glycerol dissimilation proceeds through either respiratory or fermentative pathways depending on the nature and availability of the electron acceptors (Gonzalez et al., 2008). In the presence of external electron acceptors, glycerol is first converted to glycerol-3-phosphate (G3P) via GlpK in the respiratory branch. For aerobic respiration with oxygen as the external electron acceptor, G3P is oxidized by GlpD to DHAP (Murarka et al., 2008). Alternatively, for anaerobic respiration in the presence of other non-oxygen external electron acceptors, such as fumarate or succinate, an enzyme complex GlpABC converts G3P to DHAP (Murarka et al., 2008). Our results (Supplementary Materials) suggest that glycerol dissimilation for metabolite production in P3HA31 under the shake-flask culture conditions was primarily mediated through the respiratory branch via GlpK and GlpD with oxygen as the electron acceptor. In addition, the enzyme complex GlpABC might not be involved in glycerol dissimilation under such oxygenic culture condition. However, supplying oxygen could potentially drive dissimilated carbon flux away from the Sbm pathway, limiting the supply of propionyl-CoA for 3-HV biosynthesis. On the other hand, in the absence of external electron acceptors, glycerol dissimilation proceeds fermentatively (via GldA and DhaKLM/PtsI) with intracellular NAD^+ as the electron acceptor (Gonzalez et al., 2008). Compared to the control strain P3HA31, inactivation of any gene involved in the fermentative branch, i.e., *gldA* in P3HA31Δ*gldA*, *dhaKLM* in P3HA31Δ*dhaKLM*, and *ptsI* in P3HA31Δ*ptsI*, significantly reduced 3-HV production, but minimally affected glycerol utilization, the overall metabolite profile, and even 3-HB production. The decreased 3-HV production for these single mutants could be associated with a reduced supply of propionyl-CoA. Under this hypothesis, glycerol was dissimilated via both respiratory and fermentative branches for its conversion to propionyl-CoA though the aerobic-respiratory one via GlpK-GlpD was identified to be the major route. On the other hand, the overall 3-HV production was not limited by the aerobic-respiratory route for glycerol dissimilation since episomal overexpression of GlpD in P3HA31 did not improve 3-HV production (data not shown).

As propionyl-CoA is a key precursor for 3-HV biosynthesis, metabolic engineering strategies in this study were primarily developed to

enhance carbon flux redirection from the TCA cycle to the Sbm pathway, and succinate appeared to play a key role mediating the carbon flux redirection. In *E. coli*, succinate is formed via three oxygen-dependent pathways, i.e. (i) reductive TCA branch, (ii) oxidative TCA cycle, and (iii) glyoxylate shunt. Under anaerobic conditions, the dissimilated carbon enters the TCA cycle in the form of phosphoenolpyruvate (PEP) via carboxylation to form oxaloacetate, and then proceeds with reactions in the reductive TCA branch to generate succinate as a final product (Cheng et al., 2013). On the other hand, under aerobic conditions, acetyl-CoA derived from glycolysis enters the oxidative TCA cycle to generate succinate as a cycle intermediate (Thakker et al., 2012). We previously observed that the production of 1-propanol and propionate via the Sbm pathway was favored by anaerobic conditions and was minimal under aerobic conditions (Akawi et al., 2015; Srirangan et al., 2013), suggesting that the reversed TCA branch was the main flux contributor toward the Sbm pathway. Hence, we targeted several TCA genes encoding enzymes near the succinate node for manipulation. The cultivation results of the single mutants, i.e., P3HA31Δ*sdhA*, P3HA31Δ*aceA*, and P3HA31Δ*frdB*, further confirm the main contribution from the reverse TCA branch for the carbon flux redirection into the Sbm pathway under the standard shake-flask culture conditions. Though knocking out *sucCD* can potentially disrupt the TCA cycle in both oxidative and reductive directions, *sucCD* are not essential genes since the physiologically required succinyl-CoA can still be derived via SucAB (Yu et al., 2006). However, succinyl-CoA derived from this half oxidative TCA branch cannot be funneled into the Sbm pathway since P3HA31Δ*sucD* produced no 3-HV or odd-chain metabolites. On the other hand, 3-HV biosynthesis was observed, though in a small quantity, for the double mutant P3HA31Δ*frdB*Δ*aceA*, in which only the oxidative TCA cycle was functional to generate succinate. These results suggest that succinate could be an essential precursor for carbon flux redirection into the Sbm pathway. Knocking out *sucD* can also block the carbon flux toward succinyl-CoA from both the reductive TCA branch and glyoxylate shunt, further suggesting the critical role that SucD and its associated succinate-succinyl-CoA interconversion step played in the carbon flux redirection.

Under aerobic conditions, succinate can be generated alternatively via glyoxylate shunt (Thakker et al., 2012), which is stimulated upon transcriptional activation of the *aceBAK* operon and negatively regulated by the IclR repressor (Nègre et al., 1992; Sunnarborg et al., 1990). Compared to the control strain P3HA31, the 3-HV yield was slightly increased by the *iclR* knockout. Such minimal improvement could be associated with rather anaerobic culture conditions in shake-flasks as well as carbon flux diversion (to both oxidative and reductive directions) at the succinate node. Hence, we further prevented this flux diversion by deriving a double mutant P3HA31Δ*sdhA*Δ*iclR* such that the carbon flux from glyoxylate shunt could be completely redirected to succinyl-CoA and into the Sbm pathway. Compared to the control strain P3HA31, P3HA31Δ*sdhA*Δ*iclR* cultivated in the standard screw-cap shake-flasks had a significant increase in the yield of both 3-HV and odd-chain metabolites, suggesting successful carbon flux redirection into the Sbm pathway. Such production enhancement was even more pronounced with a reduced acetate accumulation when P3HA31Δ*sdhA*Δ*iclR* was cultivated under more aerobic conditions in the vent-cap shake-flasks. Our results suggest that the shortage of oxygen supply and associated carbon spill via acetogenesis can significantly limit 3-HV production. Hence, conducting cultivation in a bioreactor under regulated oxygenic conditions would further enhance mechanistic understanding of carbon flux redirection for developing better metabolic engineering and bioprocessing strategies toward 3-HV production. Note that glyoxylate shunt essentially provides anaplerotic reactions and is only active under aerobic conditions when cells adapt to growth on C2 compounds (e.g., acetate) (Gottschalk, 1986; Kornberg and Madsen, 1957). Our results also suggest that the Sbm pathway is metabolically active and 3-HV can be produced under both anaerobic and aerobic conditions.

Funding information

This work was supported by the following Government of Canada grants: (**1**) Natural Sciences and Engineering Research Council (NSERC) Strategic Partnership grant, (**2**) Canada Research Chair (CRC) grant, and (**3**) Networks of Centres of Excellence of Canada (BioFuelNet).

Author contributions

D.M. conceived the study, formulated research plan, coordinated research team, carried out experiments, performed result interpretation and data analysis, and drafted the manuscript. K.S., T.K., and S.K. participated in the design of the study, helped to conduct experiments, performed result interpretation and data analysis. D.A.C., M.M.Y., and C.P.C. conceived, planned, supervised, and managed the study, as well as helped to draft the manuscript. All authors read and approved the final manuscript.

Declaration of competing interest

The authors declare no competing financial interests.

Appendix A. Supplementary data

Supplementary data to this article can be found online at https://doi.org/10.1016/j.ymben.2019.11.005.

References

Akawi, L., Srirangan, K., Liu, X., Moo-Young, M., Perry Chou, C., 2015. Engineering Escherichia coli for high-level production of propionate. J. Ind. Microbiol. Biotechnol. 42, 1057–1072.
Anis, S.N.S., Mohamad Annuar, M.S., Simarani, K., 2017. In vivo and in vitro depolymerizations of intracellular medium-chain-length poly-3-hydroxyalkanoates produced by Pseudomonas putida Bet001. Prep. Biochem. Biotechnol. 47, 824–834.
Arabolaza, A., Shillito, M.E., Lin, T.-W., Diacovich, L., Melgar, M., Pham, H., Amick, D., Gramajo, H., Tsai, S.-C., 2010. Crystal structures and mutational analyses of acyl-CoA carboxylase β subunit of streptomyces coelicolor. Biochemistry 49, 7367–7376.
Baba, T., Ara, T., Hasegawa, M., Takai, Y., Okumura, Y., Baba, M., Datsenko, K.A., Tomita, M., Wanner, B.L., Mori, H., 2006. Construction of Escherichia coli K-12 in-frame, single-gene knockout mutants: the Keio collection. Mol. Syst. Biol. 2, 1–11.
Bevan, M.W., Franssen, M.C.R., 2006. Investing in green and white biotech. Nat. Biotechnol. 24, 765–767.
Biernacki, M., Riechen, J., Hähnel, U., Roick, T., Baronian, K., Bode, R., Kunze, G., 2017. Production of (R)-3-hydroxybutyric acid by Arxula adeninivorans. Amb. Express 7, 4.
Cheng, K.-K., Wang, G.-Y., Zeng, J., Zhang, J.-A., 2013. Improved succinate production by metabolic engineering. BioMed Res. Int. 2013, 1–12.
Cherepanov, P.P., Wackernagel, W., 1995. Gene disruption in Escherichia coli: TcR and KmR cassettes with the option of Flp-catalyzed excision of the antibiotic-resistance determinant. Gene 158, 9–14.
de Roo, G., Kellerhals, M.B., Ren, Q., Witholt, B., Kessler, B., 2002. Production of chiral R-3-hydroxyalkanoic acids and R-3-hydroxyalkanoic acid methylesters via hydrolytic degradation of polyhydroxyalkanoate synthesized by pseudomonads. Biotechnol. Bioeng. 77, 717–722.
Erickson, B., Nelson, J.E., Winters, P., 2012. Perspective on opportunities in industrial biotechnology in renewable chemicals. Biotechnol. J. 7, 176–185.
Federsel, H.-J., 2005. Asymmetry on large scale: the roadmap to stereoselective processes. Nat. Rev. Drug Discov. 4, 685–697.
Fischer, C.R., Tseng, H.-C., Tai, M., Prather, K.L.J., Stephanopoulos, G., 2010. Assessment of heterologous butyrate and butanol pathway activity by measurement of intracellular pathway intermediates in recombinant Escherichia coli. Appl. Microbiol. Biotechnol. 88, 265–275.
Fonseca, A.C., Lima, M.S., Sousa, A.F., Silvestre, A.J., Coelho, J.F.J., Serra, A.C., 2019. Cinnamic acid derivatives as promising building blocks for advanced polymers: synthesis, properties and applications. Polym. Chem. 10, 1696–1723.
Froese, D.S., Dobson, C.M., White, A.P., Wu, X., Padovani, D., Banerjee, R., Haller, T., Gerlt, J.A., Surette, M.G., Gravel, R.A., 2009. Sleeping beauty mutase (sbm) is expressed and interacts with ygfd in Escherichia coli. Microbiol. Res. 164, 1–8.
Gao, H.-J., Wu, Q., Chen, G.-Q., 2002. Enhanced production of d-(−)-3-hydroxybutyric acid by recombinant Escherichia coli. FEMS (Fed. Eur. Microbiol. Soc.) Microbiol. Lett. 213, 59–65.
Gibson, D.G., Young, L., Chuang, R.-Y., Venter, J.C., Hutchison, C.A., Smith, H.O., 2009. Enzymatic assembly of DNA molecules up to several hundred kilobases. Nat. Methods 6, 343–345.
Gonzalez, R., Murarka, A., Dharmadi, Y., Yazdani, S.S., 2008. A new model for the anaerobic fermentation of glycerol in enteric bacteria: trunk and auxiliary pathways

in Escherichia coli. Metab. Eng. 10, 234–245.
Gottschalk, G., 1986. Bacterial Metabolism. Springer, New York.
Haller, T., Buckel, T., Rétey, J., Gerlt, J.A., 2000. Discovering new enzymes and metabolic Pathways: conversion of succinate to propionate by Escherichia coli. Biochemistry 39, 4622–4629.
Jullesson, D., David, F., Pfleger, B., Nielsen, J., 2015. Impact of synthetic biology and metabolic engineering on industrial production of fine chemicals. Biotechnol. Adv. 33, 1395–1402.
Kornberg, H., Madsen, N., 1957. Synthesis of C4-dicarboxylic acids from acetate by a "glyoxylate bypass" of the tricarboxylic acid cycle. Biochim. Biophys. Acta 24, 651–653.
Lau, N.S., Ch'ng, D.E., Chia, K.H., Wong, Y.M., Sudesh, K., 2014. Advances in poly-hydroxyalkanoate (PHA): unraveling the development and new perspectives. J. Biobased Mater. Bioenergy 9, 118–129.
Martin, C.H., Prather, K.L.J., 2009. High-titer production of monomeric hydroxyvalerates from levulinic acid in Pseudomonas putida. J. Biotechnol. 139, 61–67.
Matsumoto, K.i., Okei, T., Honma, I., Ooi, T., Aoki, H., Taguchi, S., 2013. Efficient (R)-3-hydroxybutyrate production using acetyl CoA-regenerating pathway catalyzed by coenzyme A transferase. Appl. Microbiol. Biotechnol. 97, 205–210.
Miller, J.H., 1992. A Short Course in Bacterial Genetics: a Laboratory Manual and Handbook for Escherichia coli and Related Bacteria. Cold Spring Harbor Laboratory Press, NY.
Mori, K., 1981. A simple synthesis of (S)-(+)-sulcatol, the pheromone of Gnathotrichus retusus, employing baker's yeast for asymmetric reduction. Tetrahedron 37, 1341–1342.
Murarka, A., Dharmadi, Y., Yazdani, S.S., Gonzalez, R., 2008. Fermentative utilization of glycerol by Escherichia coli and its implications for the production of fuels and chemicals. Appl. Environ. Microbiol. 74, 1124–1135.
Nahar, L., Turner, A.B., Sarker, S.D., 2009. Synthesis of hydroxy acids of dinorcholane and 5^2-cholane. J. Braz. Chem. Soc. 20, 88–92.
Nègre, D., Cortay, J.-C., Galinier, A., Sauve, P., Cozzone, A.J., 1992. Specific interactions between the IclR repressor of the acetate operon of Escherichia coli and its operator. J. Mol. Biol. 228, 23–29.
Nielsen, J., Keasling, Jay D., 2016. Engineering cellular metabolism. Cell 164, 1185–1197.
Noyori, R., Kitamura, M., Ohkuma, T., 2004. Toward efficient asymmetric hydrogenation: architectural and functional engineering of chiral molecular catalysts. Proc. Natl. Acad. Sci. U.S.A. 101, 5356–5362.
Perez-Zabaleta, M., Sjöberg, G., Guevara-Martínez, M., Jarmander, J., Gustavsson, M., Quillaguamán, J., Larsson, G., 2016. Increasing the production of (R)-3-hydroxybutyrate in recombinant Escherichia coli by improved cofactor supply. Microb. Cell Factories 15, 1–10.
Ren, Q., Ruth, K., Thöny-Meyer, L., Zinn, M., 2010. Enatiomerically pure hydroxycarboxylic acids: current approaches and future perspectives. Appl. Microbiol. Biotechnol. 87, 41–52.
Slater, S., Houmiel, K.L., Tran, M., Mitsky, T.A., Taylor, N.B., Padgette, S.R., Gruys, K.J., 1998. Multiple beta-ketothiolases mediate poly(beta-hydroxyalkanoate) copolymer synthesis in Ralstonia eutropha. J. Bacteriol. 180, 1979–1987.
Snell, K.D., Peoples, O.P., 2009. PHA bioplastic: a value-added coproduct for biomass biorefineries. Biofuels, Bioprod. Biorefining. 3, 456–467.
Sofeo, N., Hart, J.H., Butler, B., Oliver, D.J., Yandeau-Nelson, M.D., Nikolau, B.J., 2019. Altering the substrate specificity of acetyl-CoA synthetase by rational mutagenesis of the carboxylate binding pocket. ACS Synth. Biol. 8, 1325–1336.
Spengler, J., Albericio, F., 2014. ChemInform abstract: asymmetric synthesis of α-unsubstituted β-hydroxy acids. ChemInform 45, 151–161.
Srirangan, K., Akawi, L., Liu, X., Westbrook, A., Blondeel, E.J., Aucoin, M.G., Moo-Young, M., Chou, C.P., 2013. Manipulating the sleeping beauty mutase operon for the production of 1-propanol in engineered Escherichia coli. Biotechnol. Biofuels 6, 139.
Srirangan, K., Liu, X., Akawi, L., Bruder, M., Moo-Young, M., Chou, C.P., 2016. Engineering Escherichia coli for microbial production of butanone. Appl. Environ. Microbiol. 82, 2574–2584.
Srirangan, K., Liu, X., Westbrook, A., Akawi, L., Pyne, M.E., Moo-Young, M., Chou, C.P., 2014. Biochemical, genetic, and metabolic engineering strategies to enhance coproduction of 1-propanol and ethanol in engineered Escherichia coli. Appl. Microbiol. Biotechnol. 98, 9499–9515.
Sunnarborg, A., Klumpp, D., Chung, T., LaPorte, D.C., 1990. Regulation of the glyoxylate bypass operon: cloning and characterization of iclR. J. Bacteriol. 172, 2642–2649.
Taroncher-Oldenburg, G., Nishina, K., Stephanopoulos, G., 2000. Identification and analysis of the polyhydroxyalkanoate-specific β-ketothiolase and acetoacetyl coenzyme A reductase genes in the cyanobacterium synechocystis sp. strain PCC6803. Appl. Environ. Microbiol. 66, 4440–4448.
Thakker, C., Martínez, I., San, K.-Y., Bennett, G.N., 2012. Succinate production in Escherichia coli. Biotechnol. J. 7, 213–224.
Toshiyuki, C., Takeshi, N., 1987. A new synthetic approach to the carbapenem antibiotic PS-5 from ethyl (S)-3-Hydroxybutanoate. Chem. Lett. 16, 2187–2188.
Tseng, H.-C., Harwell, C.L., Martin, C.H., Prather, K.L., 2010. Biosynthesis of chiral 3-hydroxyvalerate from single propionate-unrelated carbon sources in metabolically engineered E. coli. Microb. Cell Factories 9, 96.
Tseng, H.-C., Martin, C.H., Nielsen, D.R., Prather, K.L.J., 2009. Metabolic engineering of Escherichia coli for enhanced production of (R)- and (S)-3-Hydroxybutyrate. Appl. Environ. Microbiol. 75, 3137–3145.
Weber, A.L., 1991. Origin of fatty acid synthesis: thermodynamics and kinetics of reaction pathways. J. Mol. Evol. 32, 93–100.
Welton, T., 2015. Solvents and sustainable chemistry. Proc. R. Soc. A Math. Phys. Eng. Sci. 471, 1–26.
Williams, P.D., Perlow, D.S., Payne, L.S., Holloway, M.K., Siegl, P.K.S., Schorn, T.W., Lynch, R.J., Doyle, J.J., Strouse, J.F., 1991. Renin inhibitors containing conformationally restricted P1-P1' dipeptide mimetics. J. Med. Chem. 34, 887–900.
Yazdani, S.S., Gonzalez, R., 2007. Anaerobic fermentation of glycerol: a path to economic viability for the biofuels industry. Curr. Opin. Biotechnol. 18, 213–219.
Yu, B.J., Sung, B.H., Lee, J.Y., Son, S.H., Kim, M.S., Kim, S.C., 2006. sucAB and sucCD are mutually essential genes in Escherichia coli. FEMS (Fed. Eur. Microbiol. Soc.) Microbiol. Lett. 254, 245–250.
Zheng, Z., Gong, Q., Liu, T., Deng, Y., Chen, J.-C., Chen, G.-Q., 2004. Thioesterase II of Escherichia coli plays an important role in 3-hydroxydecanoic acid production. Appl. Environ. Microbiol. 70, 3807–3813.